농학석사 학위논문

Improving Knock In efficiency in mouse generation and Biomarker discovery for Irritable Bowel Syndrome

유전자 적중 마우스 제작 효율 향상 및 IBS 바이오 마커 발굴 연구

2017 년 2 월

서울대학교 대학원
국제농업기술학과 경제동물산업기술트랙
장 다 은

Improving Knock In efficiency in mouse generation and Biomarker discovery for Irritable Bowel Syndrome

Da-Eun jang

(Supervisor: Su-Cheong Yeom, D.V.M. PhD.)

Graduate School of International Agricultural Technology

Seoul National University

Abstract

Animal model is an essential tool for studying human disease and assessing newly developing drug. Almost animal model has been developed by chemical induction or genetic modification.

The past few years have witnessed remarkable development of sequence-specific DNA endonuclease technologies in model organisms for precise genome editing, which holds the promise to greatly improve the understanding of developmental biology and diseases. Considering cost, design, and efficiency, the CRISPR/Cas9 system has a number of advantages over zinc-finger or TALE protein-fused nucleases. CRISPR/Cas9 system presented high efficiency in knock out (KO), but showed still low efficiency in knock-in (KI)-mediated gene modification. Recently, many studies for improving nuclease-mediated KI efficiency have been reported. Non-homologous end joining (NHEJ) inhibitor such as Scr7 and RS-1 induced 2~4 fold higher frequency, and single strand oligodeoxynucleotide (ssODN) modification with 3' end phosphorothioate or methyl-CpG also showed significant increase of homology direct repair (HDR) efficacy. Different with previous studies, I focus on sgRNA design and inhibitory pathway of homologous recombination (HR) by E3 ubiquitin in G1 stage. Kelch-like ECH-associated protein 1 (KEAP1) is an E3 ubiquitin ligase, which interacts with PALB2. I hypothesized that multiple sgRNAs with similar binding site increase chance of HR, and inhibition of KEAP1

would enhance HR activity in fertile embryo. KEAP1 inhibition showed relatively higher KI efficiency than control (35.7% versus 23.9%) in 110 bp (loxp-multiple cloning sequence-loxp2272) nucleotide insertion into mouse Rosa26 locus, and founder mice with precise KI was produced by microinjection. In further study for generating UPF1 loxp floxed mice, sgRNA with overlapping binding site enhanced about three fold higher KI efficiency than non-overlapped sgRNAs, and KEAP1 inhibition also increased KI rate. Most of all, combination of overlapping sgRNA and KEAP1 inhibition dramatically increase KI rate from 0% to 35.7% in mouse generation which contain single nucleotide polymorphism (cC260T in Morc2a gene). This work demonstrates that overlapping sgRNA and KEAP1 inhibition improve precise KI efficiency in three different experiments, and it would be useful for generating KI animals.

Next, I studied about animal model for human Irritible bowel syndrome (IBS). IBS is a prevalent chronic functional bowel disorder characterized by visceral hyperalgesia, abdominal pain, diarrhea and constipation without any structural cause. Although IBS is not fatal, it worsens to a patient's quality of life, and affects approximately 10–20% of world's population. B6 littermate pups were separated for 3 hours during postnatal days 3-14 or left undisturbed with their dam. Neonatal Maternal Separation (NMS) treatment induced neonatal stress, and it was confirmed by tyrosine hydroxylase (TH) gene expression in adrenal cortex. C57BL/6 mice with NMS showed IBS-D type in water contents analysis (NMS vs control: 14.67% vs 7.65% at 12weeks), but did not show growth retardation. There were no remarkable inflammation lesion in NMS and control mice of every strain

in histological examination such as H&E and immunohistochemistry for F4/80, Gr1, CD3 and mast cell chymase. In addition, quantitative PCR for detecting mRNA of Toll-like receptors (TLRs) and inflammatory cytokine genes also did not show significant difference between NMS and control mice. Strong *c-kit* and nNOS expression was detected in interstitial cell of cajal (ICC) in NMS-treated mice, but control mice showed none or weak *c-kit* expression. This might indicate that NMS mediated stress induce ICC stimulation, and followed increasing of visceral motor activity. To confirm role of nNOS in NMS-derived IBS model, B6.nNOS-/- was subjected to NMS treatment, and showed opposite results with that of B6. B6 NMS-treated $nNOS^{-/-}$ pups showed IBS-C like phenotype in feces test (NMS vs control: 7.76% vs 11.96% at 18 weeks). C57BL/6 with NMS seemed to be good model for human IBS-D, and nNOS deficient mice with NMS could be useful as IBS-C animal model. The most important finding is high *c-kit* and nNOS expression in NMS group and it might be hall marker of stress induced ICC stimulation.

In conclusion, I successfully established method for high-KI efficiency with overlapping sgRNA, and discover good bio-marker for IBS.

Key words: Animal model, CRISPR/Cas9, IBS, Knock-in, Overlapping

Student number: 2015-20012

Table of Contents

Abstract……..……..i

Table of Contents…….….iv

List of Tables…….....v

List of Figures……...vi

Part I: Improving Knock In efficiency in mouse generation

1. Introduction……..…..1
2. Material and method……..……5
3. Results……..…..8
4. Discussion……25

Part2 : Biomarker discovery for Irritable bowel syndrome

1. Introduction……..……28
2. Material and method……30
3. Results…….....38
4. Discussion……...…….47

References……49

국문초록…….54

List of Tables

Table 1. Primers for quantitative PCR…….....……34

Table 2. mAb information in histological analysis……..36

List of Figures

Figure 1. Precise 110 bp insertion into Rosa26 locus……..10

Figure 2. 110 bp insertion into mouse R26 locus…….12

Figure 3. Dual loxp insertion for conditional mice generation……..15

Figure 4. Loxp sequence insertion into UPF1 gene……17

Figure 5. Sequence alignment in *UPF1* target region……19

Figure 6. Single nucleotide polymorphism with overlapping sgRNAs and KEAP1 RNAi…….21

Figure 7. Single nucleotide substitution in *Morc2a* gene……23

Figure 8. Sequence alignment in *Morc2a* target region……..24

Figure 9. Neonatal maternal separation test……...31

Figure 10. Schematic for assessing NMS mediated IBS…….32

Fig 11. Analysis of phenotype and inflammatory genes expression……..40

Fig 12. Whole gastrointestinal transit test……...43

Fig13. Analysis of *c-kit*, nNOS and Ano1 immunohistochemistry…….44

Fig14. nNOS expression in colon tissues from NMS treated B6 mice……...46

PART I

Improving Knock In efficiency in mouse generation

1. Introduction

Technologies for making and manipulating DNA have enabled advances in biology ever since the discovery of the DNA double helix. The site-directed zinc finger nucleases (ZFNs) and TAL effector nucleases (TALENs) using the principles of DNA-protein recognition were developed. However, these systems have difficulties of protein design, synthesis, and validation remained a barrier to widespread adoption of these engineered nucleases [1].

More recently, the field of biology is experiencing a transformative phase with the advent of facile genome engineering in animals and plants using RNA-programmable system which is called clustered regularly interspaced short panlindromic repeats/ CRISPR associated protein 9 (CRISPR-Cas9). CRISPR-Cas9 is an adaptive immune defense mechanism used by Archea and bacteria for the degradation of foreign genetic material. In these organisms, the foreign genetic material from a bacteriophage is acquired and integrated into the CRISPR locus [2, 3]. This system recognizes specific sequence site and guides to direct cleavage of complementary DNA via the nuclease activity of CRISPR-Cas protein [4, 5].

Especially, the Streptococcus pyogenes Cas9 (SpCas9) is widely used for genome editing, and it mediated gene targeting with single guide RNA (sgRNA) or pair of CRISPR RNA (crRNA) and trans-activating crRNA (tracrRNA) with adequate protospacer adjacent motif (PAM) [6]. CRISPR/Cas9 system shows high

activity and recognition fidelity, so it is used in many field of research such as seed development, animal model generation and therapeutic approach [7].

CRISPR/Cas9 mediates double strand break (DSB) on target sites, and DSB induces repair process such as non-homologous end joining (NHEJ) or homologous direct repair (HDR). NHEJ is an error-prone repair and develop insertion and deletion (indel), thus it could be applicable for inducing targeted deletion or disruption of gene function. HDR is a precise repair pathway, and is useful for developing specific point mutation or exogenous DNA insertion by homologous recombination (HR) [8]. HR is a repairing process of damaged DNA before mitosis. After DSB happened, 5' to 3' resection produces 3' single strand DNA (ssDNA), which is followed by invasion of 3' ssDNA overhang into homologous sequence [9]. Several factors involve in HR pathway, mostly Rad51 recombinase develops break-induced replication, and BRAC1-PALB2-BRAC2 complex interacts with Rad51 and enhances D-loop formation and 3' ssDNA invasion [10]. HDR repair is mostly happened in S and G2 phase, and HR is suppressed by inhibition of BRCA1-PALB2-BRCA2 complex assembly by E3 ubiquitin in G1 stage [11].

Recently, many studies for improving nuclease-mediated knock-in (KI) efficiency have reported. NHEJ inhibitor such as Scr7 and RS-1 induced 2~4 fold higher HDR frequency [12, 13], and single strand oligodeoxynucleotide (ssODN) modification with 3' end phosphorothioate or methyl-CpG also showed significant increase of HDR efficacy [14, 15]. Different with previous studies, I studied for sgRNA design and inhibitoty pathway of HR by E3 ubiquitin in G1 stage. Kelch-like ECH-associated protein 1 (KEAP1) is an E3 ubiquitin ligase, which interacts with PALB2 [16]. Thus I hypothesized that inhibition of KEAP1 expression would enhance HR activity in fertile embryos. In addition, I found that multiple sgRNAs with similar binding site (overlapping sgRNA) would improve knock-in efficiency.

To verify this, sgRNAs with overlapping binding site and KEAP1 siRNA were co-transfected into one cell stage embryo or mammalian cell line, and the efficiency of NHEJ and KI was analyzed. This work demonstrates that overlapping sgRNA improves precise KI efficiency, and it would be applicable for generating KI animals.

2. Materials and Method

2.1. Animal

C57BL/6 (B6) mice were obtained from Koatech (Pyeongtaek, Korea). All mice were maintained in individual ventilated cages and were given access to feed and water *ad libitum*. This study was approved by the Institutional Animal Care and Use Committee of Seoul National University, and was conducted in accordance with approved guideline.

2.2. Preparation of Cas9, sgRNA, ssODN and KEAP1 RNAi

Cas9 mRNA was purchased from Toolgen INC (Seoul, Korea). sgRNA for each gene were designed by chopchop [17], and synthesized using in vitro RNA synthesis kit (Thermo Fisher Scientific, Waltham, MA, USA) after PCR amplification. ssODNs were designed and synthesized with commercial service (IDT, San Jose, CA, USA). 3' end of ssODN was modified with phosphorothioate to improve stability of ssODN [14]. Detail sequences of sgRNAs and ssODNs were in supplementary informations. KEAP1 siRNA was designed and synthesized by Bioneer (Daejeon, Korea) as sequence of ATCGATCGATCGATCG with 5' phosphorylation.

2.3. Microinjection into embryos

C57BL/6 female mice were super-ovulated by injection of pregnant male's serum gonadotropin and human chorionic gonadotropin, and embryos were collected at next day. After 1~2 hour incubation, normal and fertile embryos with 2

pronucleus were selected and microinjection was conducted by micromanipulator (Eppendorf, Hamburg, Germany). Briefly, 50ng/μl of Cas9 mRNA, 20~30ng/μl of sgRNAs, 20ng/μl ssODN and 10pmol/μl KEAP1 siRNA were mixed and microinjected into embryos. Embryos were cultured to 2-cell stage and transferred into pseudopregnant female, or were cultured until morula or blastocyst stage for genotyping.

2.4. Cell culture and sequencing

NIH3T3 (ATCC® CRL-1658TM) cell line was cultured in Dulbecco's Modified Eagle Medium (DMEM) with high glucose (WelGene, South Korea) supplemented with 10% fetal calf serum (WelGene) and 1X penicillin/streptomycin (WelGene). For transfection, the mixture of 4 μg of Cas9 proteins (ToolGen, South Korea) and different sgRNAs (1 μg each) with or without ssODNs (5 g) were incubated at room temperature for 5 minutes. 2 x 105 cells were then electroporated with the Cas9-sgRNA mixtures using Neon electroporator (Thermo Fischer Scientific) with 10 μL electroporation tips. After 72 hours, transfected cells were harvested and their genomic DNAs were extracted using genomic DNA purification kit (GeneAll).

2.5. Genotyping and sequencing

DNA was extracted from embryos of morula or blastocyst, and toe clips of pups. Single embryos were moved to 150μl tube with 20 μl DW by mouth pipet, and used as template for PCR after 3 times freezing/thawing and denaturation at 95 ºC for 15 minutes. DNA extraction from toe clip was conducted by commercial

extraction kit. Sequencing was conducted with conventional TA cloning and sanger sequencing.

2.6. Deep sequencing

On-target regions were PCR amplified from genomic DNA extracted from transfected cells using Phusion polymerase taq (New England Biolabs). These PCR amplicons were then subjected to paired-end deep sequencing using Mi-seq (Illumina). Data from deep sequencing were analyzed using online Cas-Analyzer (www.rgenome.net; [18]) Indels at the 3 bp upstream from the PAM sequence were considered to be mutations resulting from the reaction of CRISPR/Cas9. For HDR analyses, KIs were counted when specific donor sequences from different ssODNs were found in the read sequences.

.

2.7. Statistical analysis

For statistical analysis, t-test and chi-square ($\chi 2$ analysis) were conducted with Graphpad Prism (Graphpad software, La Jolla, CA, USA). $\chi 2$ analysis was used to calculate p-value of KI efficiency between overlapping and non-overlapping sgRNAs in embryos and pups and KEAP1 RNAi and control group. t-test was used to calculate p-values of KI efficiency in the experiments with NIH3T3 cell line. Significant differences were defined as $p<0.05$.

3. Results

3.1. KEAP1 inhibition induced relative high KI efficiency in targeted 110 nt sequence insertion into Rosa26 locus

Type II Cas9/CRISPR system with ssODN was used for generating 110bp KI into mouse Rosa26 locus. Two sgRNAs were used for increasing NHEJ and KI efficiency. The ssODN was designed to harbor 45 nt homology arms, 34 nt loxp, 42 nt multiple cloning site and 34 nt loxp2272 (Fig. 1a).

In embryo experiment, KEAP1 inhibition by siRNA induced significantly high KI efficiency (p=0.0031), but low developmental rate to morula (MO) or blastocyst (BL). KEAP1 inhibition group showed 38.1% (16/42) of KI rate and it was higher than that of control group (25.3%, p=0.0031, 17/67) (Fig. 1c). Eight pups were produced after embryo transfer, and only 3 pups from KEAP1 inhibition group were confirmed as KI (60%, 3/5). PCR and sequencing result revealed that all KI founder pups was heterozygote or mosaic phenotype (Fig. 1c). There was simultaneous NHEJ and HDR, but no pup with partial insertion or unexpected indel when KI was occurred (Fig. 1d). This result suggested that large sized 110bp sequences could be inserted successfully with ssODN into Rosa26 locus, and KEAP1 inhibition seemed to enhance efficiency for KI mouse generation. Detail schematic, sequence for ssODNs and sgRNAs were shown in Fig. 2.

The KI rate in Rosa26 locus seemed to be higher than expectation, and it is assumed that sgRNA combination with overlapping binding site might attribute this improvement. Therfore, the efficacy of the KEAP1 inhibition for precise KI

appears to have positive correlation, but it is still necessary additional tests to confirm this result.

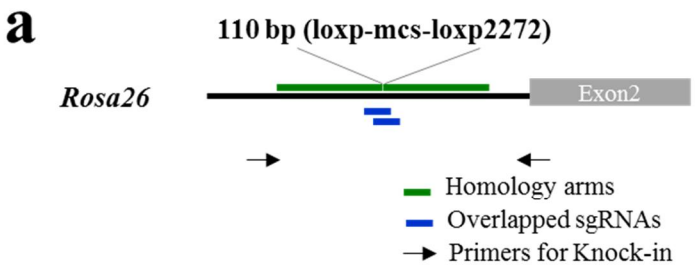
a
110 bp (loxp-mcs-loxp2272)
Rosa26
Exon2
Homology arms
Overlapped sgRNAs
Primers for Knock-in

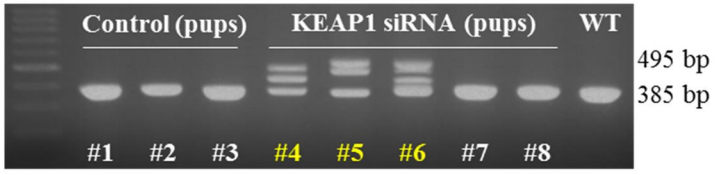
b
Control (pups)
KEAP1 siRNA (pups)
WT
495 bp
385 bp
#1 #2 #3 #4 #5 #6 #7 #8

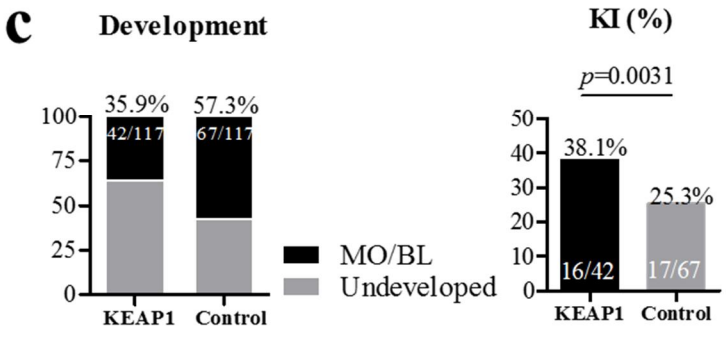
c
Development
35.9%
42/117
57.3%
67/117
100
75
50
25
0
KEAP1
Control
MO/BL
Undeveloped
KI (%)
p=0.0031
50
40
30
20
10
0
38.1%
16/42
25.3%
17/67
KEAP1
Control

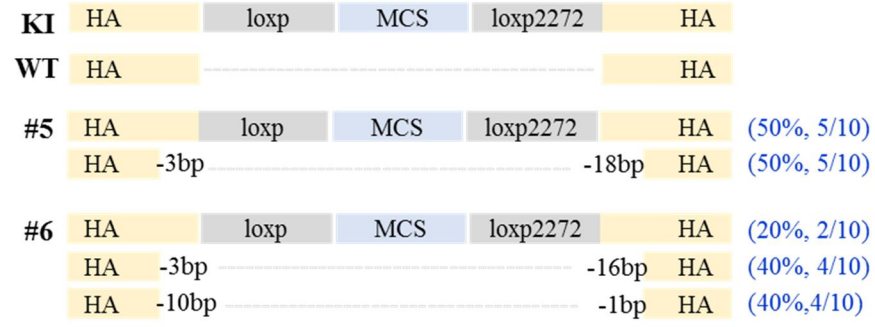
d
KI HA loxp MCS loxp2272 HA
WT HA HA
#5 HA loxp MCS loxp2272 HA (50%, 5/10)
HA -3bp -18bp HA (50%, 5/10)
#6 HA loxp MCS loxp2272 HA (20%, 2/10)
HA -3bp -16bp HA (40%, 4/10)
HA -10bp -1bp HA (40%,4/10)

Figure 1. Precise 110 bp insertion into Rosa26 locus

a) Schematic showed strategy for precise KI with ssODN including 45 nt homology sequence and 110 nt insertion sequence. 110 nt insert was consisted with 34 nt of loxp, 34 nt loxp2272 and multiple cloning site. Target site was intron 1 region of Rosa26 locus. **b)** Three days after microinjection, developmental rate and percent of KI was calculated and compared between KEAP1 siRNA treated and control group in embryos. Development (%) indicated percent of Morula (MO) or Blastocyst (BL) in total microinjected embryos. KI(%) indicated ratio of KI embryos from total MO or BL. **c)** Genotyping was conducted by PCR with specific primer, (WT: 385 bp and KI: 495 bp) in pups. **d)** Sequencing results of 3 founder pups from KEAP1 siRNA treated group. Frequency of each sequences (blue letters) were shown as number of clones / total examined clones.

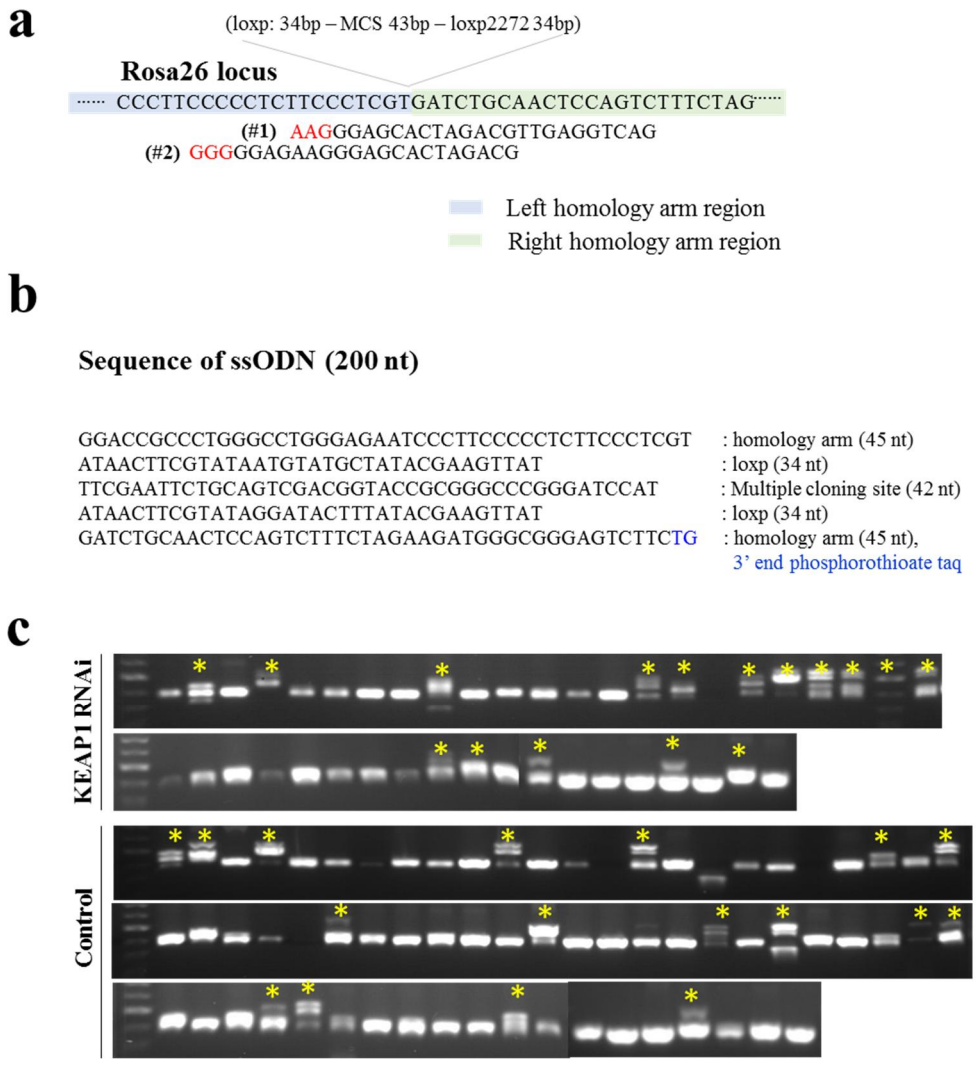

Figure 2. 110 bp insertion into mouse R26 locus

a) Brief information for sgRNA sequence and binding site. Red letter indicate PAM. b) ssODN was consisted as 45nt homology arms, loxp sequences and multiple cloning site. Blue letter indicate 5' and 3' end phosphorothioate modification. c) Genotyping by PCR with blastocyst with specific primers. * indicate knock in.

Thus, I conducted further studies for assessing influence of overlapping sgRNA and KEAP1 inhibition on HDR mediated KI.

3.2. Overlapping sgRNA increase HDR efficiency in loxp floxed and SNP KI

The other applications for precise gene targeting with ssODN are generation of single nucleotide polymorphism (SNP) and loxp sequence insertion. Conditional knock out (cKO) is essential for developing tissue specific KO mice. For producing cKO mice, 34 bp loxp sequence should be inserted into 2 different site of same gene. In other word, high HDR efficiency was essential for successful cKO mice generation. *UPF1 regulator of nonsense transcripts homolog (UFP1)* gene was designated as target and sgRNAs were designed to bind at around exon 2. To compare KI efficient between of sgRNA combination, overlapping and non-overlapping sgRNAs were transfected into NIH3T3 cell line and microinjected into 1-cell stage embryos (Fig. 3a). The detail sequence of ssODN and sgRNAs were shown in Fig.4. As expect, overlapping sgRNA developed small sized deletion, and non-overlapping sgRNA developed simultaneous large sized and small sized deletions (Fig. 3b). It was very interesting that overlapping sgRNAs developed high indel rate than non-overlapping sgRNAs (p=0.0054), and KEAP1 inhibition did not present any difference in NHEJ (Fig. 3c). These results were different with expectation, because I thought that overlapping sgRNAs would compete binding site between them. All sgRNAs in non-overlapping sgRNA group showed cleavage activity. In detail, half of the NHEJ was happened by activity with single sgRNA with small deletion size (black arrow in Fig. 3b), and the other NHEJ was developed by 2 or 3 sgRNAs (red and blue arrow in Fig. 3b).

Pattern of DSB by overlapping sgRNA presented much small and close to target site than that of non-overlapping sgRNAs (Figure 5). These results suggest that overlapping sgRNA developed high rate of DSB with small sized DSB around the target gene SNP. However, additional KI analysis exhibited too low KI rate as 0.1~0.2%, thus it was difficult to analyze. In embryo experiment, KEAP1 inhibition improved KI efficiency than control group, but not statistically significant. Compared to KEAP1 inhibition, the overlapping sgRNA combination deveolped significantly higher KI efficiency than non-overlapping sgRNAs group (p=0.0001), and there was almost 2-fold higher KI frequency (Fig. 3e). Briefly, KI test with *UPF1* gene reveal that overlapping sgRNA developed higher DSB and HDR mediated KI, but KEAP1 inhibition did not exhibit reproducible efficiency.

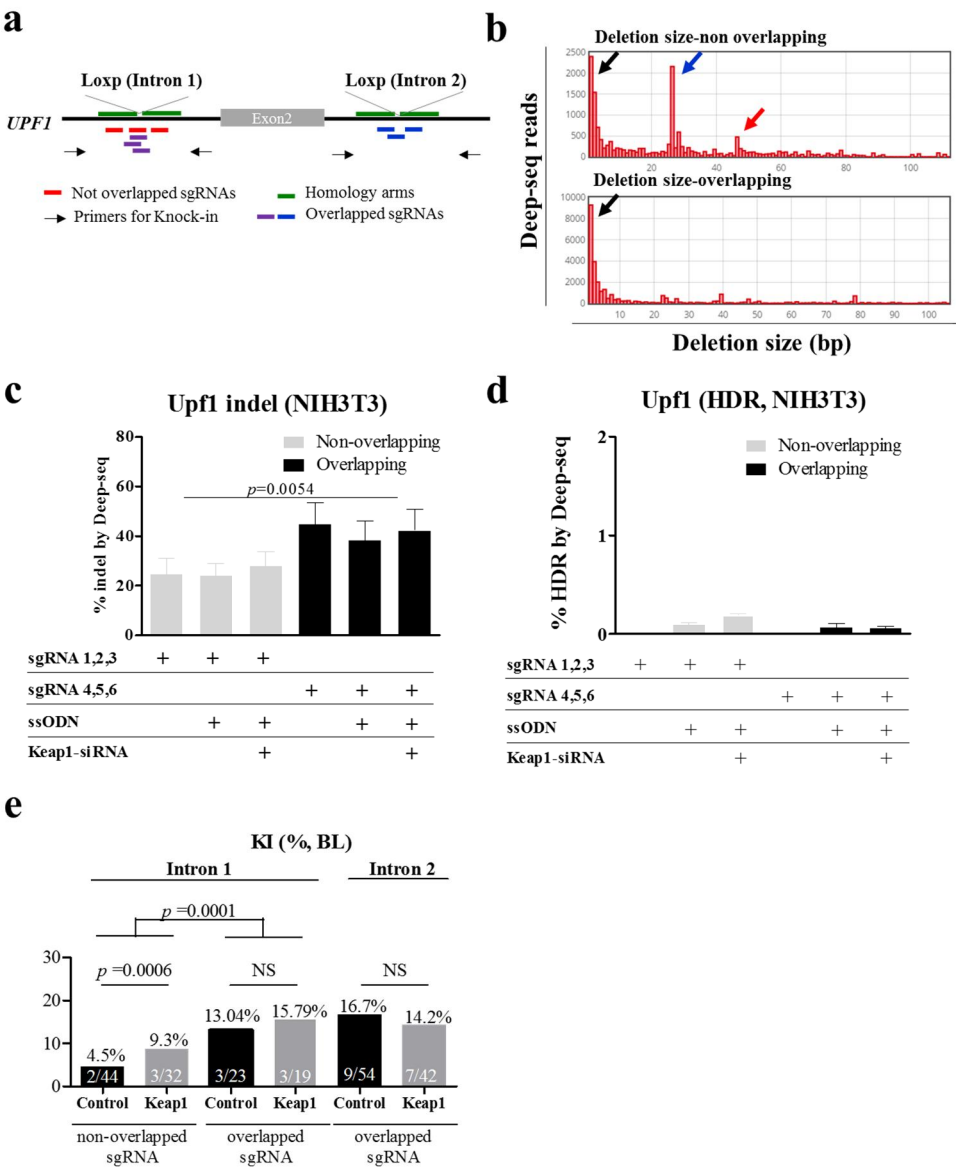
a
Loxp (Intron 1)
Loxp (Intron 2)
UPF1
Exon2
Not overlapped sgRNAs
Homology arms
Primers for Knock-in
Overlapped sgRNAs
b
Deletion size-non overlapping
Deletion size-overlapping
Deep-seq reads
Deletion size (bp)
c
Upf1 indel (NIH3T3)
Non-overlapping
Overlapping
p=0.0054
% indel by Deep-seq
sgRNA 1,2,3
sgRNA 4,5,6
ssODN
Keap1-siRNA
d
Upf1 (HDR, NIH3T3)
Non-overlapping
Overlapping
% HDR by Deep-seq
sgRNA 1,2,3
sgRNA 4,5,6
ssODN
Keap1-siRNA
e
KI (%, BL)
Intron 1
Intron 2
p =0.0001
p =0.0006
NS
NS
4.5%
2/44
9.3%
3/32
13.04%
3/23
15.79%
3/19
16.7%
9/54
14.2%
7/42
Control
Keap1
Control
Keap1
Control
Keap1
non-overlapped sgRNA
overlapped sgRNA
overlapped sgRNA

Figure 3. Dual loxp insertion for conditional mice generation

a) Schematic showed brief strategy for cKO mice generation with ssODN in *UPF1* gene. For gene targeting in intron 1 region of *UPF1* gene, 2 different combination of sgRNAs were used as non-overlapping (red bar) and overlapping (purple bar) sgRNAs. In case of intron 2, partial overlapping sgRNAs were used. ssODN was consist with 48 nt homology arm and 104 nt of insert sequence with loxp and mutation especially in PAM sequence of sgRNA binding site. b) Distribution of clones with various sized deletion in overlapping and non-overlapping sgRNAs group. Bar indicate the counted cell number in each deletion size. Arrow indicate the gathering of similar deletion size. Each arrow indicate small deletion by single sgRNA (sgRNA #1, #2 or #3, black arrow), moderate deletion by dual sgRNA (sgRNA #1 and #2 or #2 and #3, blue arrow) and large deletion (red arrow). c and d) Three days after transfection with sgRNA, ssODN and keap1 siRNA into NIH3T3 cell line, rate of NHEJ (indel) and HDR (KI) were calculated by deep-sequencing. *p* value was calculated with *t*-test and $p<0.05$ indicate significantly difference e) KI rate was calculated by PCR with specific primers. *p* value was calculated with $\chi 2$ analysis and $p<0.05$ indicate significantly difference.

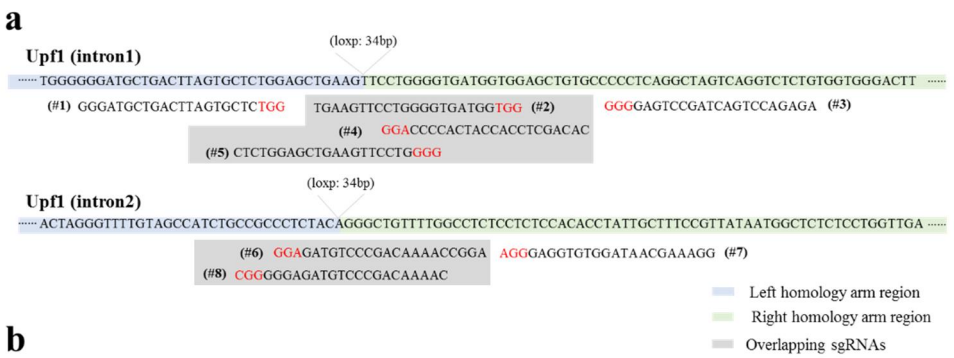

b

Sequence of ssODN in Upf1 intron 1 (200 nt)

GCTACTTCTAGGCTCCTGAAGAACCCGGTGGCTAAGTGTTGGGTGGA	: homology arm (48 nt)
TGCTGACTTAGTGCTCTATAGCTGAAG	; homology arm with mutation in PAM sequence
ATAACTTCGTATAGCATACATTATACGAAGTTAT	: loxp (34 nt)
TTCCTGGGGTGATGATTAAGCTGTGCATACTCAGGCTAGTCAGG	: homology arm with mutation in PAM sequence
TCTCTGTGGTGGGACTTCAGTGCAGACATCCTATGCTGTGACTTTGAG	: homology arm (48 nt) with 3' end phosphorothioate taq

Sequence of ssODN in Upf1 intron 2 (200 nt)

ACCCACACACACACCCAGCAAGGCCAGAGCTTGTCTTTACTAGGGTTTTGTAGCCATCTG	: homology arm (60 nt)
CGCCGCACTA	: homology arm with mutation in PAM sequence (10 nt)
ATAACTTCGTATAGCATACATTATACGAAGTTAT	: loxp (34 nt)
CAGGGCTGTTTTGGCCTCTCGACTCCACACCTATTGCTTTCC	: homology arm with mutation in PAM sequence (42 nt)
GTTATAATGGCTCTCTCCTGGTTGACAAGTGTTTTCGAGGATAAAACCAGAGC	: homology arm (53 nt) with 3' end phosphorothioate taq

c

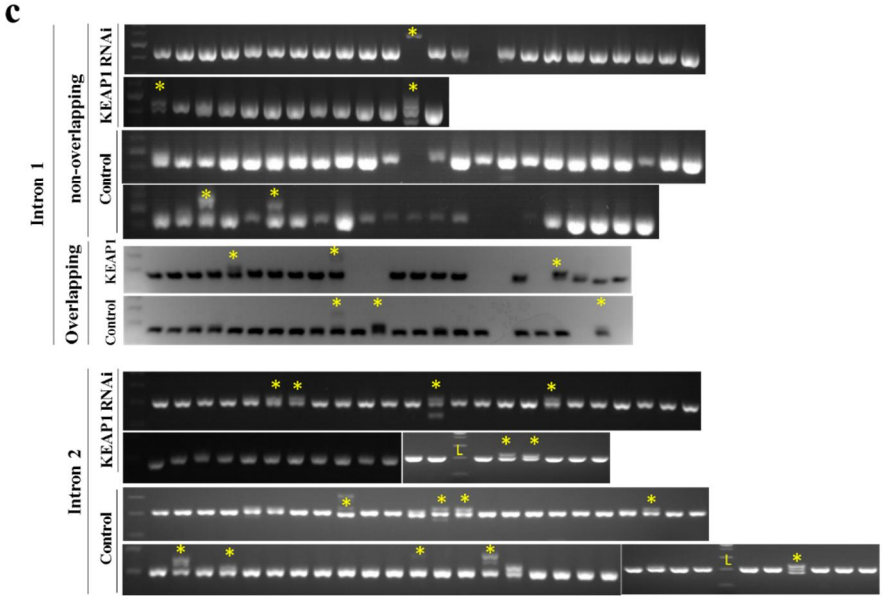

Figure 4. Loxp sequence insertion into UPF1 gene

a) Brief information for sgRNA sequences and binding site. Red letter indicate PAM. b) ssODN was consisted as homology arms and loxp sequence. Red letters indicate nucleotide alteration for preventing DSB after KI, and Blue letter indicate 5' and 3' end phosphorothioate modification. c) Genotyping by PCR with blastocyst. * indicate knock in, and L indicate ladder.

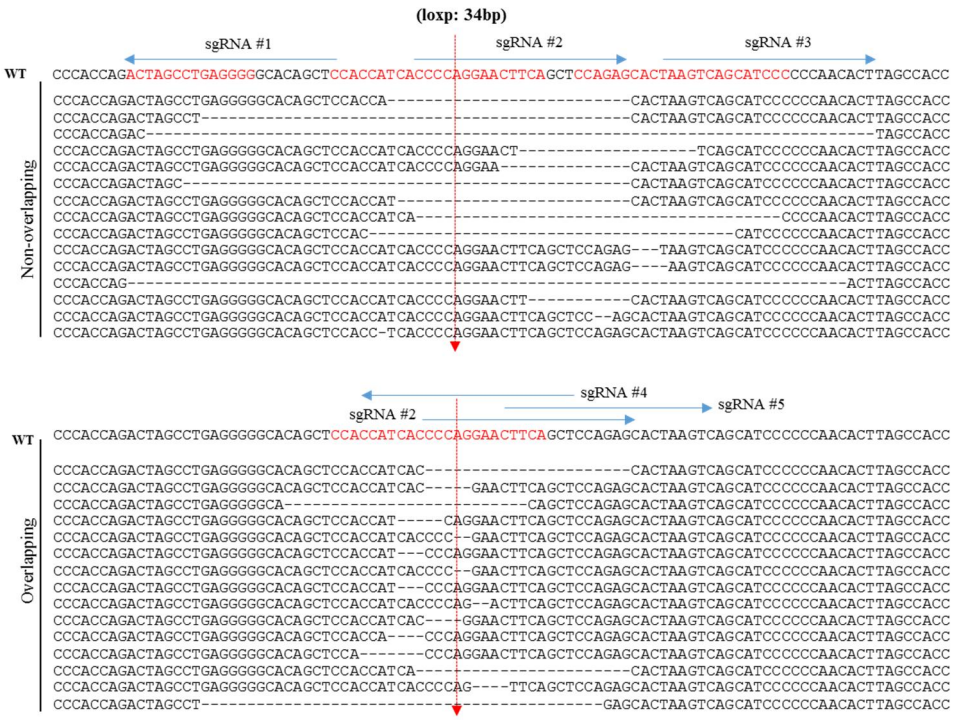

Figure 5. Sequence alignment in *UPF1* target region

Fifteen DSB patterns were analyzed and aligned. Red spell indicate sgRNA binding site, and red arrow indicate target site for SNP.

To confirm the influence of overlapping sgRNA and KEAP1 inhibition, additional study for SNP modification with *Microrchidia 2A* (*Morc2a*) gene was conducted using NIH3T3 cell and embryo. SNP with cytosine to thymine in 260th coding sequence (cC260T) changed amino acid translation as serine to leucine (pS87L). For precise genetic editing, ssODN was designed harboring silent mutation and 60bp homology arms. Two groups of sgRNAs were designed as overlapping and non-overlapping binding site (Fig. 6a). Overlapping sgRNA developed similar NHEJ rate and deletion size with non-overlapping sgRNAs in transfection test with NIH3T3 cell (Fig. 6b, 6c and Fig. 7). In analysis for HDR mediated KI rate, overlapping sgRNA developed about 2 fold higher KI rate than non-overlapping sgRNA in NIH3T3 cell (Fig. 6d and Fig. 8). On following embryo experiment, non-overlapping sgRNA induced almost 0% of KI efficacy in control and KEAP1 inhibition group. However, overlapping sgRNA induced 35.7% and 44.4% of KI in KEAP1 inhibition and control groups, and it was significantly different ($p < 0.0001$) (Fig. 6e and fig. 7c). Although, overall KI rate was higher in embryo than cells as about 20-fold, it was consistent that overlapping sgRNA enhanced higher rate of KI.

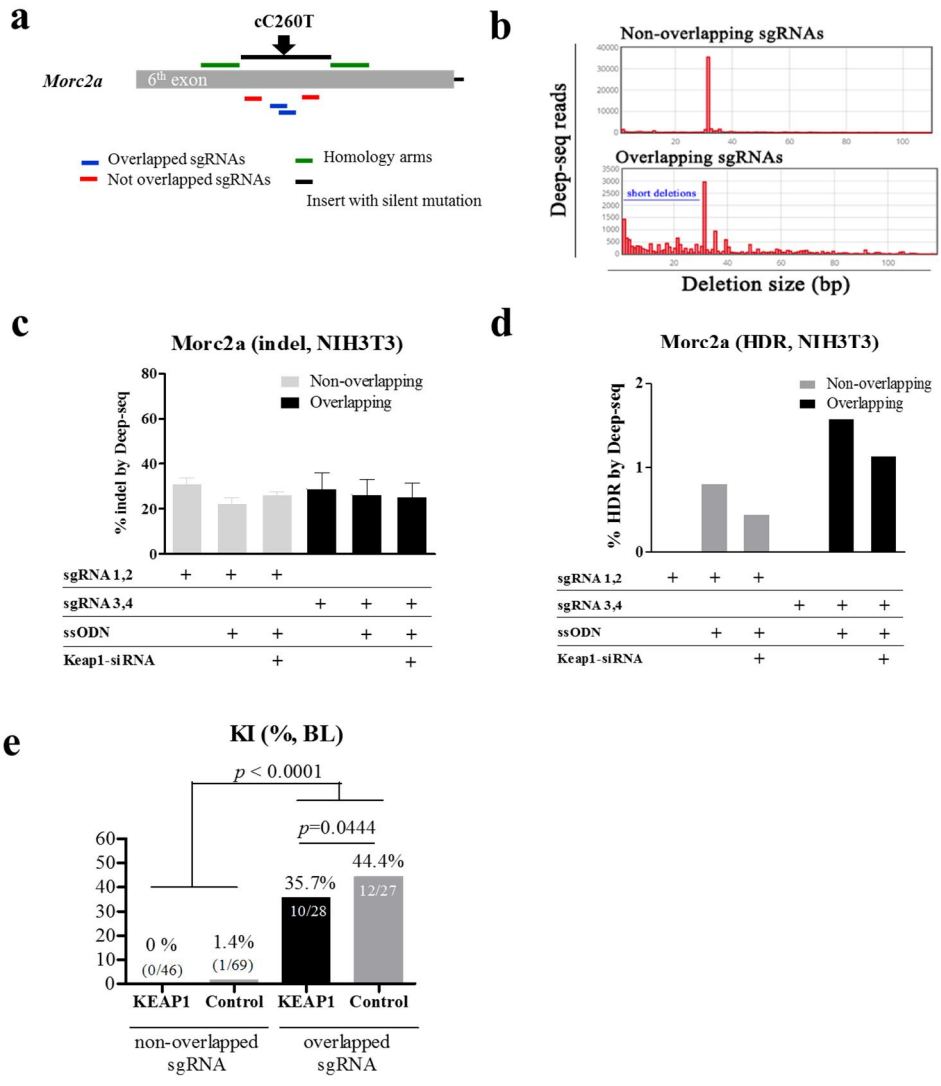
a
cC260T
Morc2a
6th exon
Overlapped sgRNAs
Not overlapped sgRNAs
Homology arms
Insert with silent mutation
b
Non-overlapping sgRNAs
Overlapping sgRNAs
short deletions
Deep-seq reads
Deletion size (bp)
c
Morc2a (indel, NIH3T3)
% indel by Deep-seq
Non-overlapping
Overlapping
sgRNA 1,2
sgRNA 3,4
ssODN
Keap1-siRNA
d
Morc2a (HDR, NIH3T3)
% HDR by Deep-seq
Non-overlapping
Overlapping
sgRNA 1,2
sgRNA 3,4
ssODN
Keap1-siRNA
e
KI (%, BL)
p < 0.0001
p=0.0444
0 %
(0/46)
1.4%
(1/69)
35.7%
10/28
44.4%
12/27
KEAP1
Control
KEAP1
Control
non-overlapped sgRNA
overlapped sgRNA

Figure 6. Single nucleotide polymorphism with overlapping sgRNAs and KEAP1 RNAi

a) Schematic showed strategy for producing cC260T SNP in Morc2a gene with Cas9, sgRNAs and ssODN. ssODN was consist with 60nt of homology arm and 45nt of insert with silent and targeted mutation. b) Distribution of clones with various sized deletion in overlapping and non-overlapping sgRNA group. Bar indicate the counted cell number in each deletion size. c and d) After transfection with sgRNAs, ssODN and KEAP1 siRNA transfection into NIH3T3 cell line, and indel and HDR rate was analyzed by deep sequencing. Bar indicate by percent of indel and HDR. e) KI rate in embryo was shown as percent (%, number of KI BL / total survived BL). *p* value was calculated by chi-square ($\chi 2$) analysis.

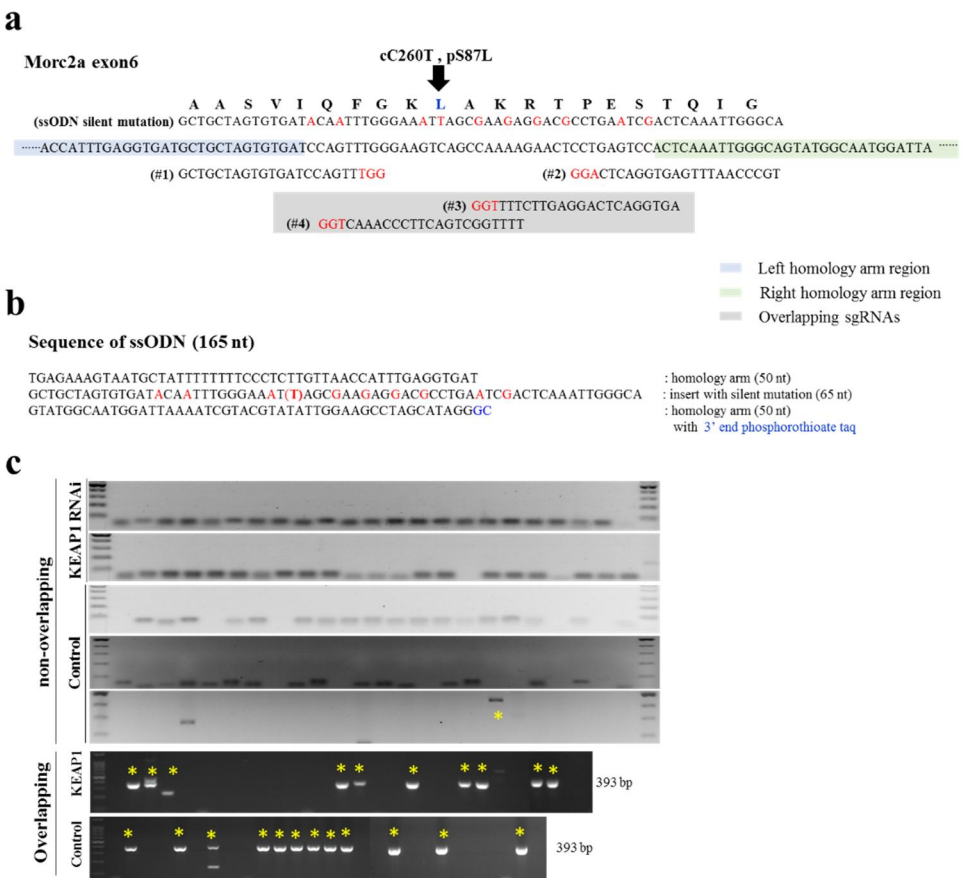

Figure 7. Single nucleotide substitution in *Morc2a* gene

a) Brief information for sgRNA sequences and binding site. Red letter indicate PAM. b) ssODN was consisted as 50 nt homology arms and insert sequences with silent mutation. Bold letter indicate target nucleotide for SNP (cC260T) and red letters indicate nucleotides for silent mutation. Blue letter indicate 5' and 3' end phosphorothioate modification. c) Genotyping by PCR with blastocyst. * indicate knock in.

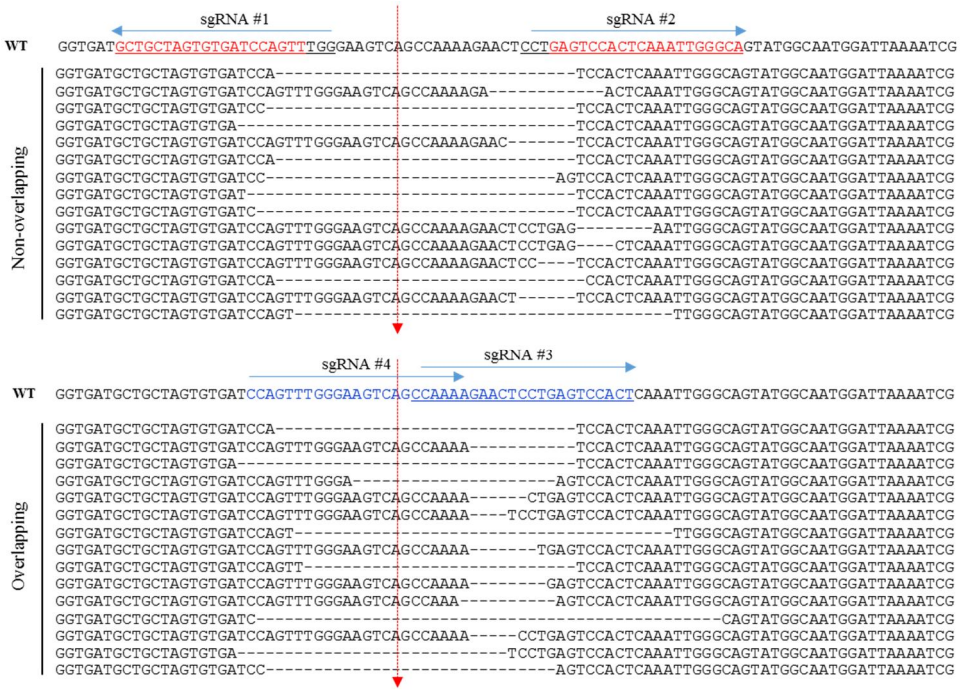

Figure 8. Sequence alignment in *Morc2a* target region

Fifteen DSB patterns were analyzed and aligned. Red and blue spell indicate sgRNA binding site, and red arrow indicate target site for loxp sequences insertion.

4. Discussion

CRISPR/Cas9 system is an efficient tool for developing DSB and consequential HDR, mediated precise KI. Precise gene targeting is efficient tool for KI animal and cell establishment, and these are applicable for correction of genetic errors. Even though some reports presented high KI efficiency with CRISPR/Cas9 [12-14], there was still controversy for low efficiency of HDR-mediated KI [19]. Thus, there is still needs of further study for improving KI efficiency [20].

For improving KI efficiency, I focused on initial stage of HDR such as DSB, resection and strand invasion [9]. At first, I studied about KEAP1, which repress BRCA1-PLAB2-BRCA2 complex formation during G1 stage cell and cause suppress HR [21]. Even though, KEAP1 inhibition seemed to improve KI rate in several cases of embryo experiment, it was not statistically significant. Indeed, KEAP1 inhibition caused embryo toxicity. As previous report, KEAP1 inhibition could improve KI rate under 53BP1 inhibition [21]. Taken together, it is concluded that sore inhibition of KEAP1 would fail for significantly improving the KI efficiency in mice embryo.

Next aspect for improving KI efficiency was DSB for initiating HR. Masafumi et al [22] reported that there was weak correlation between DSB frequency and KI efficiency. Indeed, co-injection of Cas9 protein and mRNA was helpful for generating KI [23]. Based on the previous studies, I assumed that frequency of DSB is important, but specific DNA region-focused deletion with small sized deletion would be more influential than DSB frequency. To develop small sized deletion covering target sequence, I designed overlapping sgRNA. My study with

overlapping sgRNA using cell demonstrated that overlapping sgRNA did not affect indel efficiency, and it induced small sized deletion close to the intended mutation region. Recently, Dominik et al. suggested that small deletion close to target sequence is good enough for precise KI in in vitro experiment [20]. Current study also demonstrated highly positive correlation between KI and overlapping sgRNA. In every case of embryo test with various overlapping and non-overlapping sgRNA exhibited significantly higher KI rate with more than 2 fold increase. Following study for KI mice generation, every case showed high KI rate for introducing foreign sequence into target regions. These results assure that, overlapping sgRNA system is very efficient and simple way for precise gene targeting through CRISPR/Cas9 and ssODN mediated gene targeting.

Additional considerable point is interaction between sgRNAs. Because each sgRNA was designed to bind the same strand, they would compete the binding site. If sgRNAs were designed from different strand, there could be a chance of dimer formation between among sgRNAs, which might interfere the DSB frequency. It was turned out that the overlapping sgRNAs from same strand did not reduce DSB frequency (3 genes with 4 target insertions). Interaction between sgRNAs is still uncertain, but overlappings sgRNA designed to bind any strand seemed work well.

Taken together, this work suggests potential solution for improving KI efficiency. Overlapping sgRNA could produce small sized deletion close to target sequence, and this improves KI efficiency significantly. With this system, I successfully generated several KI with SNP and conditional mice without failure. Moreover, overlapping sgRNA system is very simple, so it could be applicable many other gene editing field easily.

PART II

Biomarker discover for Irritable bowel syndrome

1. Introduction

Irritable bowel syndrome (IBS) is a functional gastrointestinal (GI) disorder with changing normal bowel movements with an estimated prevalence of 10–20% [24]. Clinical symptoms of IBS include abdominal pain or discomfort, stool irregularities and bloating, as well as other somatic, visceral and psychiatric comorbidities [25]. Although not life-threatening, it is a heavy economic burden due to increased work absenteeism and impaired quality of life of its sufferers, as well as increased use of health care services [26].

The pathophysiology of IBS is not complete understand due to the lack of a clearly identified pathological abnormality and reliable biomarkers. However, possible cause of IBS might be physical stressors, infection, inflammation, psychological disorder such as anxiety, depression, and significant negative events [24]. A distinguishing feature of IBS is that symptoms, including visceral sensitivity, are often triggered or continued stress [27]. Stress would disrupts homeostasis, and develop such as alterations in intestinal motility, visceral perception, gut barrier function. Recently, there has been an increasing interest in the neural and immunological networks related stress within the gut and the bi-directional communication [28-32]. The autonomic nervous system (ANS) and the hypothalamus-pituitary-adrenal (HPA) axis are commonly regarded as the major components of the stress response system by releasing related stress hormone [33]. These systems are supposed to induce changes in gastrointestinal functions and could possibly link psychological states to gastrointestinal symptoms such as pain, diarrhea, constipation [34, 35]. Therefore, there is still need for investigation about

alterations of intestinal motility and visceral sensitivity induced by psychological stress.

Early traumatic experiences such as childhood neglect, abuse, loss of a parent, and life-threatening situations during childhood have been shown to increase the risk of IBS development [36, 37]. Consequently, many investigators have attempted to develop animal models of stressful experience in childhood and, postnatal handling, early separation and daily periodic Neonatal maternal separation (NMS) have been proposed. .

The NMS model was used the majority of studies of brain-gut dysfunction to mimic stress induced human IBS [38, 39]. And, they showed induced motility changes in the GI, visceral hypersensitivity or associated alterations in the functioning of the HPA axis. [30, 39-42]. The model is based on the premise that changes to the environment during the early postnatal period can have long lasting enduring effects into adulthood. These effects include altered stress responsivity such as increased visceral pain perception and GI motility [30].

In this study, I generate IBS animal model that was induced by NMS stress, and assessed factors related to brain-gut interation such as stress factors and colonic motility factors such as ICC, and nNOS. This study offers some important insights into alterations of intestine motility factors such as Interstitial cells of cajal (ICC) and nNOS. As a result, I found novel marker for IBS to assess the gastrointestinal motility factors in IBS mouse that were induced by NMS stress.

2. Materials and Method

2.1. Animal and neonatal maternal separation

Male and female C57BL/6 were purchased from Koatech (Pyeongtaek, Korea). During postnatal days (PND) 3 to 14, half of pups were separated from their maternity cages and were exposed to a 180-min period of daily maternal separation [43]. During separation, pups were

under a lamp to keep them warm at 37℃. After separation, pups were returned to their maternity cages. Control groups were maintained in their maternity cages with the dams without any separation stress [44]. Animals were housed on a 12:12-h light-dark cycle with access to food and water **ad libitum**. Litters were weaned on day 21. This study was approved by the Institutional Animal Care and Use Committee of Seoul National University, and was conducted in accordance with approved guideline.

2.2. Fecal parameters measurements.

NMS and control pups were placed in clean transparent cages with wire mesh individually and allowed access to their standard lab chow and tap water ad libitum. Then, feces from each mouse were collected, counted and weighted. The number and weight of feces were expressed in terms of the total number and wet weight per mouse. After weighted, the wet feces for each mouse were dried at 105°C for 48 h. The water content of feces was calculated as :

$$\text{fecal water content (\%)} = \frac{(feces\ weight\ before\ dried - feces\ weight\ after\ dried)}{feces\ weight\ before\ dried} \times 100$$

[45]

Figure 9. Neonatal maternal separation test

Randomly selected pups were separated from maternal cage, and kept in separated container with warm condition. After 8 hours, the separated pups were returned to maternal cage.

PND	Day 3 – 14	Day 21	Wk 4	Wk 5	Wk 6	Wk 7	Wk 8	Wk 9	Wk 10	Wk 11	Wk 12	After samping
NMS	O											qPCR, IHC, Western blotting
Body weight	O	O	O	O	O	O	O	O	O	O	O	
Feces test					O						O	
WGI			O									

Figure 10. Schematic for assessing NMS mediated IBS

NMS were conducted during PND 3~14, and all pups including were weaned at 21 days old. Fecal parameters measurement was performed at 6 weeks and 12 weeks old. After second fecal sampling, all mice were euthanized and colon tissues were collected.

2.3. Necropsy and sampling

After 12weeks, all mouse were euthanized, and samples were collected. In detail, adrenal gland and colon tissues from proximal, transverse and distal region, were obtained and stored in formalin or deep freezer after dipping in RNAlater (Ambion, MA, USA) for 12 hours at 4℃.

2.4. Quantitative polymerase chain reaction

Total RNA was isolated from mouse colon using Trizol reagent according to manufacturer's specifications (Ambion). cDNA was synthesized by using RNA to cDNA synthesis kit (ThermoFisher). Each sample was diluted as same concentration of 10ng/μl. Quantitative RT-PCR was conducted with 3μl of cDNA, 10μl of SYBR pcr premix (ThermoFisher) and 0.2μl of specific primers (100μM). All reactions were performed in quadruple in an Step one plus system (ThermoFisher), and thermal cycling conditions were 10min at 95℃, followed by 40 cycles of 95℃ for 15s, 60℃for 1min, and one more cycle for confirming melt curve. The sequences of specific primers were shown in Table 1. Gene expression was normalized with that of GAPDH.

Table1. Primers for quantitative PCR

Target gene	Genbank Accession		Sequence(5' to 3')	tm	size
TLR1	NM_030682	F	TGAGGGTCCTGATAATGTCCTAC	61	153
		R	AGAGGTCCAAATGCTTGAGGC		
TLR2	NM_011905	F	GCAAACGCTGTTCTGCTCAG	61	231
		R	AGGCGTCTCCCTCTATTGTATT		
TLR4	NM_021297	F	ATGGCATGGCTTACACCACC	61	129
		R	GAGGCCAATTTTGTCTCCACA		
TLR5	NM_016928	F	GCAGGATCATGGCATGTCAAC	62	130
		R	ATCTGGGTGAGGTTACAGCCT		
TLR7	NM_133211	F	ATGTGGACACGGAAGAGACAA	60	207
		R	GGTAAGGGTAAGATTGGTGGTG		
Tyrosine Hydroxylase	NM_009377	F	GTGCCAGAGAGGACAAGGTTC	60	130
		R	CGATACGCCTGGTCAGAGA		
MCP1	NM_011333.3	F	TTAAAAACCTGGATCGGAACCAA	60	121
		R	GCATTAGCTTCAGATTTACGGGT		
IL-1b	NM_008361	F	GAAATGCCACCTTTTGACAGTG	60	116
		R	TGGATGCTCTCATCAGGACAG		
GAPDH	NM_008084	F	AGGTCGGTGTGAACGGATTTG	61	123
		R	TGTAGACCATGTAGTTGAGGTCA		

2.5. Histological examination

Formalin fixed tissues from colon were used for immunohistochemistry. For immunohistochemistry, rabbit anti-mouse *c-kit*, nNOS and Ano were used for primary antibodies. Detail information for primary antibodies and dilution condition were shown in Table 2. Following primary antibody incubation, the sections were rinsed for 5min each in PBS for three times and then incubated for 1h in a biotinylated secondary antibody (*c-kit* : 1:200 goat serum in PBS; Ano1 : 1:200 rabbit serum in PBS; nNOS 1:2000 goat serum in PBS; F4/80 1:200 goat serum in PBS; mastcell chymase 1:200 goat serum in PBS) at RT. Following incubation in the solution containing avidin-biotin complex (Vectastain Elite ABC kit, Vector Laboratories,MA, USA) for 30min at RT and subsequently reacted with diamino-benzidine (DAB, Vector Laboratories, MA, USA), sections were counterstained using haematoxylin. Sections were mounted on permount medium (permount 1: xylene1), dehydrated in a series of graded ethanol and cover slipped.[44]

2.6. Whole gastrointestinal transit test

All mice were fasted overnight (18h) before experiments, animals treated with 300ul of carmine marker(Sigma, Saint Louis, USA). Then animals transferred to the cage that its bottom was covered with white sheet. First observation of defecated marker recorded as a whole gut transit time[46]

Table 2. Antibody information in histological analysis

	target	Clone	HOST	Dilution	company
Primary antibody	a-tubulin	11H10	Mouse	1 : 3000 (WB)	CST
	Ano1	S-20	Goat	1 : 100 (IHC)	Santa cruz
	c-kit	C-19	Rabbit	1 : 100 (IHC), 1 : 500 (WB)	Santa cruz
	nNOS	nos1	Goat	1 : 3000 (WB)	abcam
	F4/80	BM8	rat	1 : 100 (IHC)	abcam
	mast cell chymase	CMA1	Rabbit	1 : 100 (IHC)	biorbyt
Secondary Antibody	Goat anti rabbit		Goat	2 fold dilution ratio of primary antibody	Santa cruz
	Goat anti rat		Goat		Santa cruz
	Goat anti mouse		Goat		Santa cruz
	Rabbit anti goat		Rabbit		Santa cruz

2.7. Western blotting

Tissues from NMD and control mice were dissected out and lyzed in 200μl of RIPA buffer(iNtRON, Gyeonggi, Korea) containing proteinase inhibitor for 4h at 4℃. Then, tissues lysates were centrifuged 13,000rpm for 30min at 4℃. The concentration of protein in homogenate was determined using a BCA protein assay kit (ThermoFisher). Thirty micrograms of proteins were loaded onto a 8% SDS-PAGE gel. After electrophoresis, the proteins were electro transferred onto polyvinyldifluoride (PVDF) membranes (Millipore, Massachusetts, USA) at 100V for 2h at 4℃. The membranes were incubated in 10ml of blocking buffer (1x TBS and 5% w/v non-fat milk) for 1h at room temperature. Goat anti-mouse a-tubuline (Cell signaling technology, Danvers, USA) and Goat-anti-mouse nNOS (Santa Cruz, Santa Cruz, USA) were used for primary antibodies. After incubation, the membranes were washed with TBST (1x TBST and 0.5% tween20) three times for 5min each and incubated with anti-goat HRP-conjugated secondary antibody (1:2000; Santa Cruz) for 2h at room temperature. The membrane washed with TBST three times for 5min each. The immunoreactive proteins were detected by enhanced chemiluminescence (ECL kit; Abclon, Guro, Korea) [47].

2.8. Statistical analysis

For analysis significant difference of gene expression between control and NMS mice, *t*-test was conducted with GraphPad Prism (Graphpad software, La Jolla, CA, USA)

3. Results

3.1. NMS developed IBS-Diarrhea similar symptoms

After 12 days of NMS, general phenotype such as growth curve, fecal parameter measurement and gene expression were assessed in control and NMS mice. At first, there was no difference in growth rate between control and NMS pups (Fig. 11A), and no remarkable phenotype such as serve emaciation, pain reflex, paresis and hair loss.

To confirm, that the NMS mice were under stress situation during NMS, expression of Tyrosine hydroxylase (TH) gene in small intestine, colon and adrenal gland was compared between control and NMS groups. As shown in Fig. 11B, NMS group presented TH gene up-regulation in the intestine and adrenal gland. NMS mice showed about 2-fold times increase. In detail, there were significant difference of TH gene expression in small intestine (p=0.0054) and adrenal gland (p=0.0359). TH gene expression in large intestine, proximal colon showed relative higher gene expression than distal region. Altogether, increasing of TH gene expression indicated that NMS pups were under stressful situation.

Next, fecal parameter measurement was conducted, and percentage of water content in each groups were calculated. Only male mice showed significant difference in the percentage of water contents in 6 weeks and 12 weeks old. In addition, difference of percentage of water contents was larger in 12 weeks old NMS mice than control mice. While NMS developed difference in percentage water contents as 11.65% vs control 9.49% at 6 weeks, and NMS 14.67% vs control 7.65% at 12 weeks in male mice, developed fecal water contents difference

as 10.66% vs control 9.81% at 6 weeks of age, and NMS 9.83%vs control 7.26% at 12 weeks of age in female mice (Fig. 11c and 11d). The higher water content percentage in male NMS mice might indicate that NMS would induce diarrhea like symptom. The reason why male showed significantly different water content with age-dependent manner was not obvious, however, this result revealed that male C57BL/6 would be more sensitive than female under NMS situation.

3.2. NMS developed mild inflammation in intestine

Further study about inflammation in intestine was conducted with quantitative PCR and histological examination, and results revealed that several inflammatory genes such as TLR1, TLR2, TLR4, TLR5, IL-1b and MCP1 were relatively over-expressed than control mice. Especially, TLR4 (p=0.0365), IL-1b (p=0.0057) and MCP1 (p=0.0004) were significantly highly expressed in colon (Fig. 11E). Similarly with the gene expression pattern, there were relatively many cells with F4/80 positivity. F8/40 antigen is surface marker of macrophage cell population, and MCP1 is monocyte chemoattractant protein 1, and these results demonstrated that NMS induced inflammation like symptom. However, there was any remarkable inflammatory symptom in H&E (data not shown). Thus It is concluded that NMS would induce mild inflammation in colon.

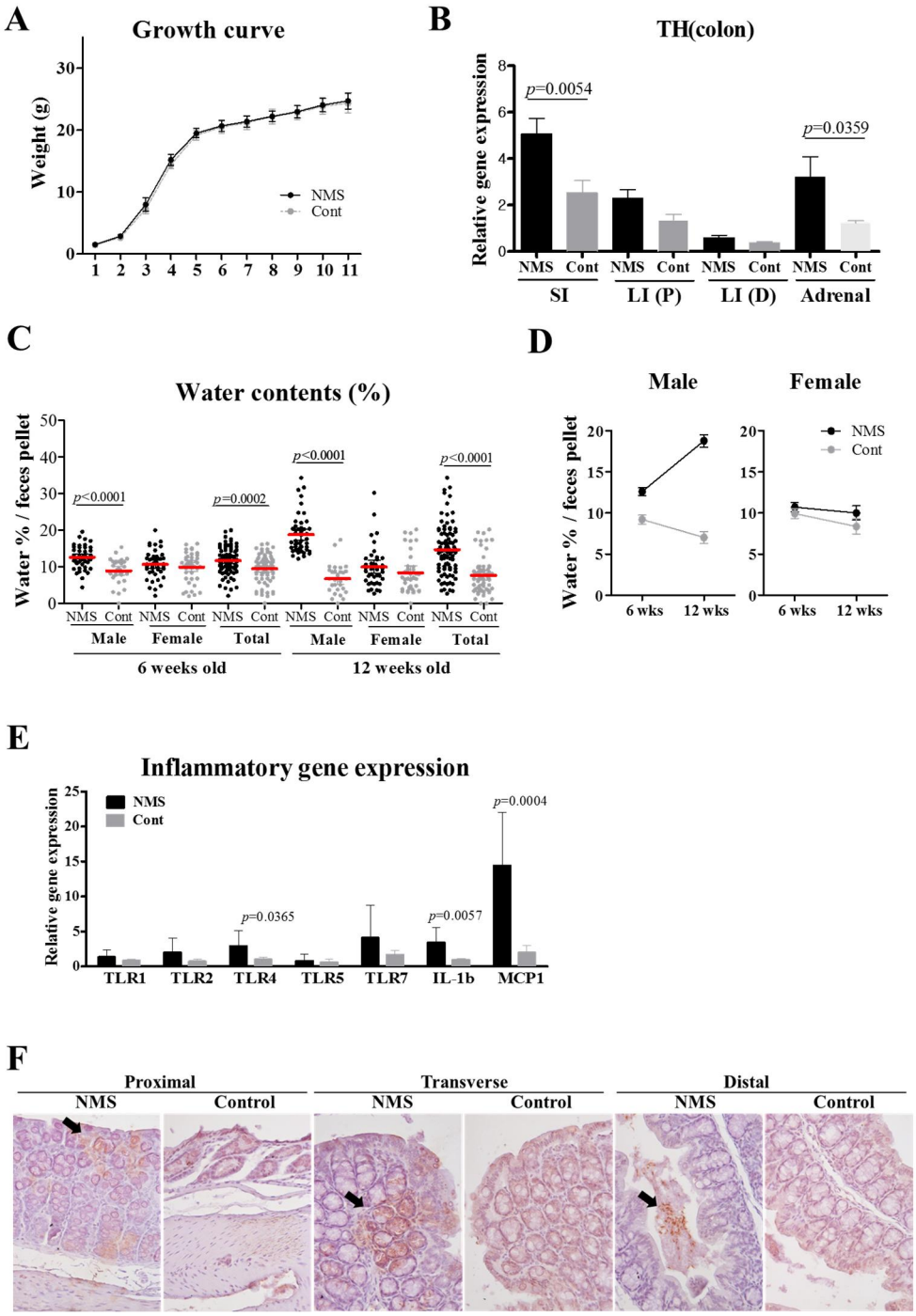
A
Growth curve
Weight (g)
NMS
Cont
B
TH(colon)
Relative gene expression
p=0.0054
p=0.0359
NMS Cont NMS Cont NMS Cont NMS Cont
SI
LI (P)
LI (D)
Adrenal
C
Water contents (%)
Water % / feces pellet
p<0.0001
p=0.0002
p<0.0001
p<0.0001
NMS Cont NMS Cont NMS Cont NMS Cont NMS Cont NMS Cont
Male
Female
Total
Male
Female
Total
6 weeks old
12 weeks old
D
Male
Female
Water % / feces pellet
NMS
Cont
6 wks
12 wks
6 wks
12 wks
E
Inflammatory gene expression
Relative gene expression
NMS
Cont
p=0.0365
p=0.0057
p=0.0004
TLR1
TLR2
TLR4
TLR5
TLR7
IL-1b
MCP1
F
Proximal
Transverse
Distal
NMS
Control
NMS
Control
NMS
Control

Fig 11. Analysis of phenotype and inflammatory genes expression

NMS mediated irritable bowel syndrome in C57BL/6 pups. a) Weight of each pups were calculated every weeks from 1 weeks to 11 weeks old. (NMS; n=10, Cont; n=10), data was shown as mean ± SEM. b) Relative gene expression of tyrosine hydroxylase (TH) were analyzed by quantitative PCR with mRNA from small intestine (SI), large intestine (LI proximal region and LI distal region), and adrenal cortex. Data were shown as mean ± SEM. c) Water contents in feces were calculated in 6 weeks old and 12 weeks old, respectively. NMS and control mice were littermate. d) The difference of water contents in feces (%) between male/female and NMS/control. Data were shown as mean ± SEM. e) Relative gene expression analysis for several inflammatory genes (TLR1, TLR2, TLR4, TLR5, TLR7, IL-1b, MCP1) in large intestine tissues from NMS and control mice. Data were shown as mean ± SEM. f) Immunohistochemistry for F4/80 in colon tissues. Arrow indicate F4/80 positive tissues.

3.3. NMS stimulate c-kit and nNOS in myenteric plexus that cause enhance gastrointestinal motility.

As shown in Fig. 11, NMS induced IBS-D type symptom, but they did not present severe inflammation, thus further examination about motor activity of intestine was conducted. At first, whole gastrointestinal transit test was conducted, and it showed NMS mice showed faster transition than that of control mice. All NMS mice showed whole gastrointestinal transit before 3 hours, but control mice showed about 2~5 hours (Fig. 12). This indicate that there was relative high visceral motor activity, and might suggest there was shorter time for water absorption in colon.

Next, further study about visceral motor activity was conducted by immunohistochemistry for various marker of intestinal cell of cajal (ICC). Two well-known ICC marker such as *c-kit* and Ano1 was used with colon tissues (proximal, transverse and distal region). As expected, *c-kit* in NMS mice was highly expressed in myenteric plexus which was supposed to be ICC, but control mice did not present remarkable expression of *c-kit*. I thought that this *c-kit* express pattern might indicate activation of visceral motor. To confirm, we conducted additional immune stain for ICC with Ano1 which is known as another marker for ICC [48], but there was no difference expression pattern between NMS and control mice. Furthermore, Ano1 positive cell was located in vili rather than visceral muscle layer (Fig. 13). This results suggest that Ano1 is not good marker for ICC in muscle layer.

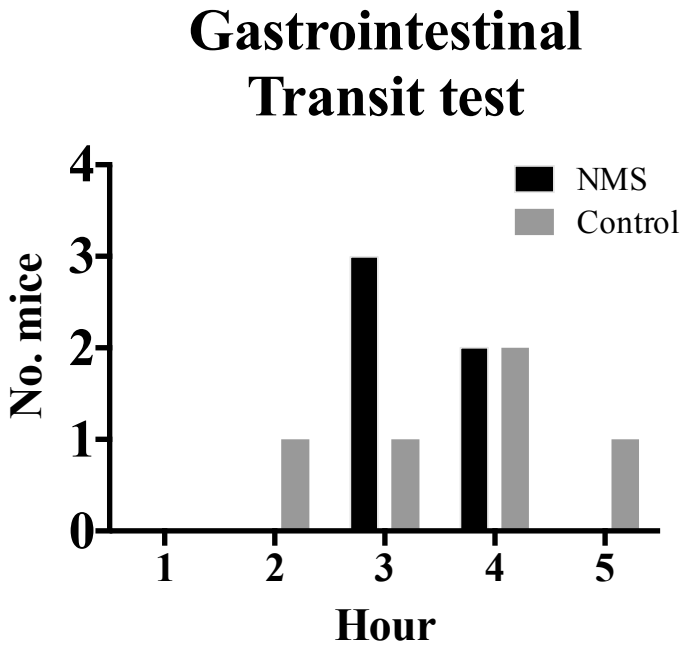

Fig 12. Whole gastrointestinal transit test

The x axis appear whole gastrointestinal transit measurement time and y axis is number of mouse. (NMS; n=5, Cont; n=5), data was shown as mean ± SEM.

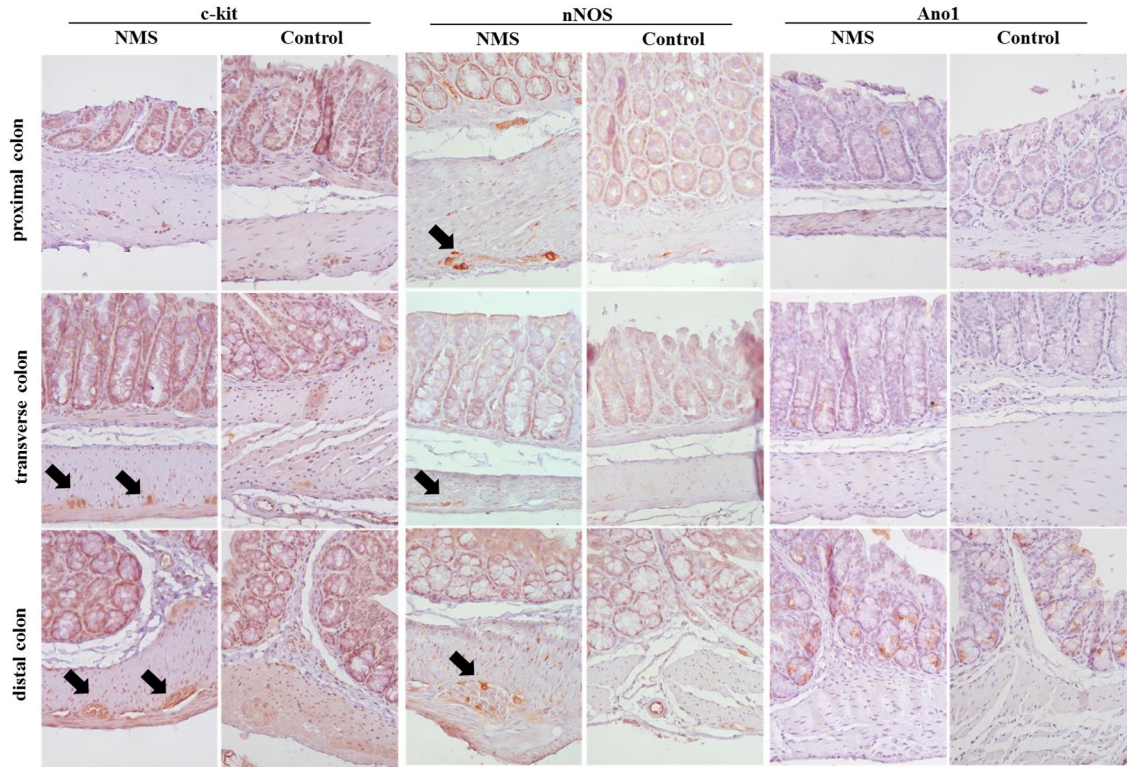

Fig13. Analysis of *c-kit*, nNOS and Ano1 immunohistochemistry

Immunohistochemistry analysis for *c-kit*, nNOS and Ano-1 in colon tissues from NMS and control mice. Colon were divided to 3 region as proximal, transverse and distal. Arrow indicate antigen expressed region (DAB stained). Magnification: 400x.

3.4. nNOS was novel biomarker for NMS induced IBS model

After ICC activation was confirmed by *c-kit* immune stain, we studied about other marker for ICC which would upregulated under NMS. There was highly expression of nNOS in muscle layer of NMS, but not in control mice. nNOS expression site was similar with that of *c-kit* expression, and this demonstrated that nNOS was another biomarker of ICC activation. It is interesting that high nNOS expression was also observed in proximal region of colon (Fig. 13).

The nNOS expression under NMS was confirmed by quantitative PCR with colon tissues. Relative nNOS gene expression was 1.502 vs 1.175 in small intestine, 0.8667 vs 0.574 in proximal colon and 0.652 vs 0.512 in distal colon (NMS versus control). Though, significant difference of nNOS gene expression was observed only in proximal colon, but nNOS showed relatively high expression also in small intestine and distal colon (Fig. 14A).

Then, additional experiment for nNOS expression in NMS was conducted with western blotting analysis. Colon with NMS only showed nNOS protein expression, but not it control mice (Fig. 14.B). Altogether these results, nNOS was novel marker of NMS mediated IBS model, and activation of nNOS would enhance visceral motor activity.

Finally, I try to elucidate activity of nNOS in IBS with NMS. To do this, B6.nNOS deficient mice (B6.nNOS$^{-/-}$) was used for NMS and its phenotype was assessed. NMS with B6.nNOS-/- showed adverse fecal parameter with that of wild type B6. As described in Fig. 11c, B6 with NMS developed IBS-D type phenotype, but B6.nNOS-/- with NMS presented IBS-constipation (IBS-C) type phenotype.

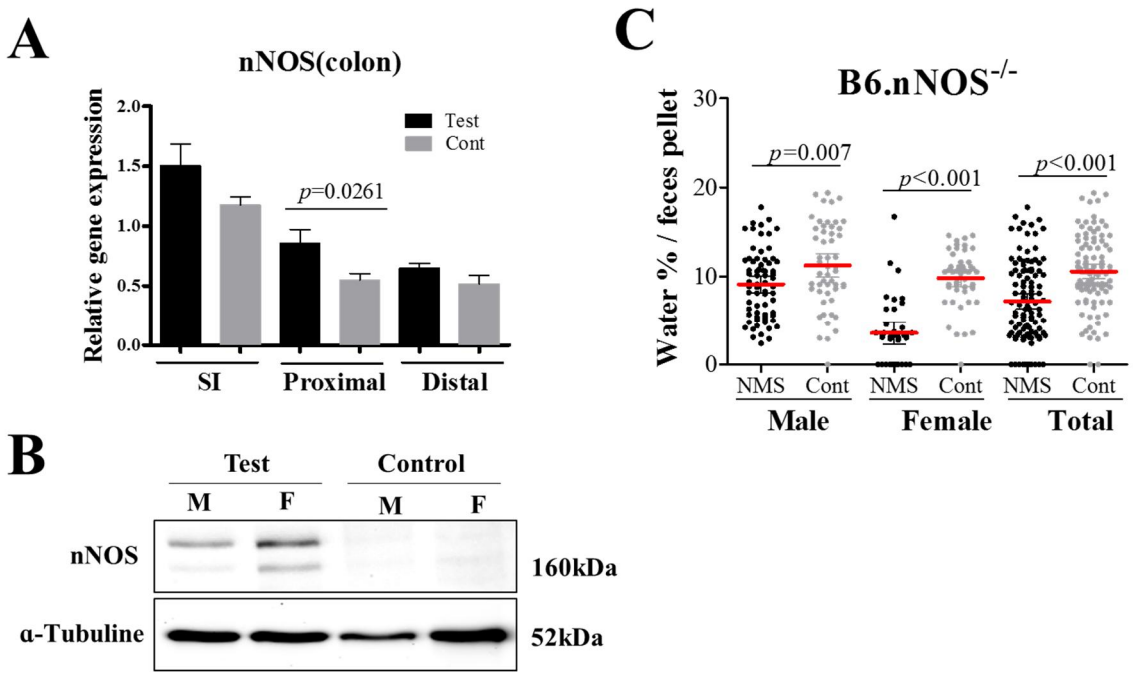

Fig14. nNOS expression in colon tissues from NMS treated B6 mice

a) nNOS gene expression was compared with colon tissues from B6 NMS and control mice. Data were shown as mean ± SEM. b) nNOS protein expression was confirmed by western blot with colon tissues from B6 NMS and control. The protein expression was normalized by a-tubuline. c) Additional NMS treat was conducted with B6.nNOS$^{-/-}$, and analyze the water contents (%) in feces.

4. Discussion

The diagnosis of IBS mainly depend on symptom-based diagnostic criteria those of Manning et al. and the Rome criteria which have been widely used to identify IBS patients. IBS is considered to be a disorder without organic colonic lesions until now [49, 50].

In this study, I successfully developed IBS model with NMS, and they showed highly similar with human IBS. This study demonstrated that NMS could be good model for neonatal stress induced human IBS with low grade inflammation, no growth retardation and diarrhea dominant phenotype [51]. However, female is known to be more sensitive in IBS, but NMS mouse model showed that male showed remarkable IBS phenotype. Nevertheless, this study demonstrate several novel biomarker such as *c-kit* and nNOS in ICC. Furthermore, I speculate symptom of IBS is related with gastrointestinal motility factors.

Especially, the *c-kit* and nNOS highly expressed in myenteric plexus from NMS induced IBS mice. The *c-kit* is known as ICC marker, and it play important roles in gastrointestinal motility [52]. ICC play as an electrical pacemaker and mediate both inhibitory and excitatory motor neurotransmissions, which manifest as electrical slow waves in smooth muscles. Consequently, ICC are necessary for maintaining gastrointestinal motility. The decrease of ICC, as observed in several motility disorders, reduces amplitudes of slow wave and, consequently, induces intestinal dysmotility by reducing electrical drive to smooth muscle contractions and peristalsis [53]. This is consistent with our observation that NMS stress activate ICC, and enhance visceral motor activity.

I also elucidated nNOS as new biomarker for IBS. Nitric oxide (NO) is a gaseous messenger which plays an essential role in the physiology and pathophysiology of the gastrointestinal tract (GI). NOS have three isoforms and nNOS is known for NO production from the distal colon of NMS rats. nNOS upregulation interact with reactive oxygen species, and contribute to the visceral hypersensitivity in IBS [54].

In this study, I successfully developed IBS mouse model with NMS, and also discovered several findings such as *c-kit* and nNOS expression related with intestinal motility from NMS mice. Thus, this study suggest that c-kit and Nnos could become a novel biomarker of IBS.

Reference

1. Doudna, J.A. and E. Charpentier, *Genome editing. The new frontier of genome engineering with CRISPR-Cas9.* Science, 2014. **346**(6213): p. 1258096.
2. Wiedenheft, B., S.H. Sternberg, and J.A. Doudna, *RNA-guided genetic silencing systems in bacteria and archaea.* Nature, 2012. **482**(7385): p. 331-8.
3. Jinek, M., et al., *A programmable dual-RNA-guided DNA endonuclease in adaptive bacterial immunity.* Science, 2012. **337**(6096): p. 816-21.
4. Liu, T., et al., *Development and potential applications of CRISPR-Cas9 genome editing technology in sarcoma.* Cancer Lett, 2016. **373**(1): p. 109-18.
5. van der Oost, J., et al., *Unravelling the structural and mechanistic basis of CRISPR-Cas systems.* Nat Rev Microbiol, 2014. **12**(7): p. 479-92.
6. Cong, L., et al., *Multiplex genome engineering using CRISPR/Cas systems.* Science, 2013. **339**(6121): p. 819-23.
7. Hsu, P.D., E.S. Lander, and F. Zhang, *Development and applications of CRISPR-Cas9 for genome engineering.* Cell, 2014. **157**(6): p. 1262-78.
8. Sander, J.D. and J.K. Joung, *CRISPR-Cas systems for editing, regulating and targeting genomes.* Nat Biotechnol, 2014. **32**(4): p. 347-55.
9. Sung, P. and H. Klein, *Mechanism of homologous recombination: mediators and helicases take on regulatory functions.* Nat Rev Mol Cell Biol, 2006. **7**(10): p. 739-50.
10. Buisson, R., et al., *Cooperation of breast cancer proteins PALB2 and piccolo BRCA2 in stimulating homologous recombination.* Nat Struct Mol Biol, 2010. **17**(10): p. 1247-54.
11. Orthwein, A., et al., *A mechanism for the suppression of homologous recombination in G1 cells.* Nature, 2015. **528**(7582): p. 422-6.
12. Song, J., et al., *RS-1 enhances CRISPR/Cas9- and TALEN-mediated knock-in efficiency.* Nat Commun, 2016. **7**: p. 10548.
13. Maruyama, T., et al., *Increasing the efficiency of precise genome editing with CRISPR-Cas9 by inhibition of nonhomologous end joining.* Nat Biotechnol, 2015. **33**(5): p. 538-42.

14. Renaud, J.B., et al., *Improved Genome Editing Efficiency and Flexibility Using Modified Oligonucleotides with TALEN and CRISPR-Cas9 Nucleases.* Cell Rep, 2016. **14**(9): p. 2263-72.
15. Bertoni, C., A. Rustagi, and T.A. Rando, *Enhanced gene repair mediated by methyl-CpG-modified single-stranded oligonucleotides.* Nucleic Acids Res, 2009. **37**(22): p. 7468-82.
16. Park, J.Y., F. Zhang, and P.R. Andreassen, *PALB2: the hub of a network of tumor suppressors involved in DNA damage responses.* Biochim Biophys Acta, 2014. **1846**(1): p. 263-75.
17. Labun, K., et al., *CHOPCHOP v2: a web tool for the next generation of CRISPR genome engineering.* Nucleic Acids Res, 2016.
18. Park, J., et al., *Cas-analyzer: an online tool for assessing genome editing results using NGS data.* Bioinformatics, 2016.
19. Oji, A., et al., *CRISPR/Cas9 mediated genome editing in ES cells and its application for chimeric analysis in mice.* Sci Rep, 2016. **6**: p. 31666.
20. Paquet, D., et al., *Efficient introduction of specific homozygous and heterozygous mutations using CRISPR/Cas9.* Nature, 2016. **533**(7601): p. 125-9.
21. Orthwein, A., et al., *A mechanism for the suppression of homologous recombination in G1 cells.* Nature, 2015.
22. Inui, M., et al., *Rapid generation of mouse models with defined point mutations by the CRISPR/Cas9 system.* Sci Rep, 2014. **4**: p. 5396.
23. Chu, V.T., et al., *Efficient generation of Rosa26 knock-in mice using CRISPR/Cas9 in C57BL/6 zygotes.* BMC Biotechnol, 2016. **16**(1): p. 4.
24. Philpott, H., P. Gibson, and F. Thien, *Irritable bowel syndrome - An inflammatory disease involving mast cells.* Asia Pac Allergy, 2011. **1**(1): p. 36-42.
25. Piche, M., et al., *Decreased pain inhibition in irritable bowel syndrome depends on altered descending modulation and higher-order brain processes.* Neuroscience, 2011. **195**: p. 166-75.
26. Shih, Y.C., et al., *Resource utilization associated with irritable bowel syndrome in the United States 1987-1997.* Dig Dis Sci, 2002. **47**(8): p. 1705-15.

27. Moloney, R.D., et al., *Stress and the Microbiota-Gut-Brain Axis in Visceral Pain: Relevance to Irritable Bowel Syndrome.* CNS Neurosci Ther, 2016. **22**(2): p. 102-17.
28. Venkova, K., et al., *Exposure of the amygdala to elevated levels of corticosterone alters colonic motility in response to acute psychological stress.* Neuropharmacology, 2010. **58**(7): p. 1161-7.
29. Fichna, J. and M.A. Storr, *Brain-Gut Interactions in IBS.* Front Pharmacol, 2012. **3**: p. 127.
30. Moloney, R.D., et al., *Early-life stress induces visceral hypersensitivity in mice.* Neurosci Lett, 2012. **512**(2): p. 99-102.
31. Tramullas, M., T.G. Dinan, and J.F. Cryan, *Chronic psychosocial stress induces visceral hyperalgesia in mice.* Stress, 2012. **15**(3): p. 281-92.
32. Piche, T., et al., *Impaired intestinal barrier integrity in the colon of patients with irritable bowel syndrome: involvement of soluble mediators.* Gut, 2009. **58**(2): p. 196-201.
33. Smith, S.M. and W.W. Vale, *The role of the hypothalamic-pituitary-adrenal axis in neuroendocrine responses to stress.* Dialogues Clin Neurosci, 2006. **8**(4): p. 383-95.
34. Jones, M.P., et al., *Brain-gut connections in functional GI disorders: anatomic and physiologic relationships.* Neurogastroenterol Motil, 2006. **18**(2): p. 91-103.
35. Lomax, A.E., K.A. Sharkey, and J.B. Furness, *The participation of the sympathetic innervation of the gastrointestinal tract in disease states.* Neurogastroenterol Motil, 2010. **22**(1): p. 7-18.
36. Hill, O.W. and J.S. Price, *Childhood bereavement and adult depression.* Br J Psychiatry, 1967. **113**(500): p. 743-51.
37. Lowman, B.C., et al., *Recollection of childhood events in adults with irritable bowel syndrome.* J Clin Gastroenterol, 1987. **9**(3): p. 324-30.
38. Barreau, F., et al., *New insights in the etiology and pathophysiology of irritable bowel syndrome: contribution of neonatal stress models.* Pediatr Res, 2007. **62**(3): p. 240-5.
39. O'Mahony, S.M., et al., *Maternal separation as a model of brain-gut axis dysfunction.* Psychopharmacology (Berl), 2011. **214**(1): p. 71-88.

40. Dorner, G., et al., *Pyridostigmine administration in newborn rats prevents permanent mental ill-effects produced by maternal deprivation.* Endokrinologie, 1981. **77**(1): p. 101-4.
41. Matthews, K., L.S. Wilkinson, and T.W. Robbins, *Repeated maternal separation of preweanling rats attenuates behavioral responses to primary and conditioned incentives in adulthood.* Physiol Behav, 1996. **59**(1): p. 99-107.
42. Mayer, E.A., et al., *Functional GI disorders: from animal models to drug development.* Gut, 2008. **57**(3): p. 384-404.
43. Ren, T.H., et al., *Effects of neonatal maternal separation on neurochemical and sensory response to colonic distension in a rat model of irritable bowel syndrome.* Am J Physiol Gastrointest Liver Physiol, 2007. **292**(3): p. G849-56.
44. Chung, E.K., et al., *Neonatal maternal separation enhances central sensitivity to noxious colorectal distention in rat.* Brain Res, 2007. **1153**: p. 68-77.
45. Zhou, M., et al., *Laxative effects of Salecan on normal and two models of experimental constipated mice.* BMC Gastroenterol, 2013. **13**: p. 52.
46. Mehri, D., et al., *EFFECTS OF BLACK TEA EXTRACT AND ITS THEARUBIGINS ON WHOLE GUT TRANSIT TIME IN MICE: INVOLVEMENT OF 5-HT3 RECEPTORS.* Jundishapur J Nat Pharm Prod, 2008(01): p. 39-44.
47. Hu, S., et al., *Sensitization of sodium channels by cystathionine beta-synthetase activation in colon sensory neurons in adult rats with neonatal maternal deprivation.* Exp Neurol, 2013. **248**: p. 275-85.
48. Loera-Valencia, R., et al., *Ano1 is a better marker than c-Kit for transcript analysis of single interstitial cells of Cajal in culture.* Cell Mol Biol Lett, 2014. **19**(4): p. 601-10.
49. Manning, A.P., et al., *Towards positive diagnosis of the irritable bowel.* Br Med J, 1978. **2**(6138): p. 653-4.
50. Thompson, W.G., et al., *Functional bowel disorders and functional abdominal pain.* Gut, 1999. **45 Suppl 2**: p. II43-7.

51. Ohman, L. and M. Simren, *Pathogenesis of IBS: role of inflammation, immunity and neuroimmune interactions.* Nat Rev Gastroenterol Hepatol, 2010. **7**(3): p. 163-73.
52. Sung, R., et al., *Interstitial cells of Cajal (ICC)-like-c-Kit positive cells are involved in gastritis and carcinogenesis in human stomach.* Oncol Rep, 2011. **26**(1): p. 33-42.
53. Jo, H.J., et al., *Fat deposition in the tunica muscularis and decrease of interstitial cells of Cajal and nNOS-positive neuronal cells in the aged rat colon.* Am J Physiol Gastrointest Liver Physiol, 2014. **306**(8): p. G659-69.
54. Tjong, Y.W., et al., *Role of neuronal nitric oxide synthase in colonic distension-induced hyperalgesia in distal colon of neonatal maternal separated male rats.* Neurogastroenterol Motil, 2011. **23**(7): p. 666-e278.

국문초록

실험 동물 모델은 인간 질병과 신약 개발 평가 연구에 기본적인 수단이다. 대부분의 동물 모델은 화학 약물이나 유전자 조작을 통해 만들어 진다.

최근 유전자 조작 동물 모델을 만드는 데 가장 많이 활용되고 있는 CRISPR/Cas9 system 은 ZFN, TALEN 보다 가격, 설계, 효율성 면에서 많은 이점을 가지고 있다. CRISPR/Cas9 system 의 높은 활성으로 인해 유전자의 Knock Out(KO) 효율이 이전보다 많이 높아진 것에 비해 Knock In(KI)에서는 여전히 낮은 효율을 보이고 있다.

그렇기 때문에 최근에는, Endonuclease 를 통해 KI 효율을 높이는 방법에 대한 연구들이 많이 이루어지고 있다. HDR 비율을 2-4 배 이상 높이도록 유도하는 방법으로 NHEJ inhibitor 인 Scr7, RS-1 이 있고, HDR 효율을 높이는 방법으로 phosphorothioate 또는 metyl CpG 을 3'말단에 붙여 조작한 단일 가닥(ssODN)을 이용한 것도 알려져 있다. 이전의 연구들과는 다르게, 이 연구에서는 sgRNA 의 설계와 G1 단계에서 E3 유비퀴틴에 의한 HR 저해 기작에 집중하였다. Kelch like ECH-associated protein1 (KEAP1) 은 E3 유비키틴 연결효소이고 PALB2 와 상호 작용한다고 알려져 있다.

즉, 타겟 위치가 비슷한 여러 개의 sgRNA(overlapping sgRNAs)를 처리하여 HR 발생을 높이고, KEAP1 을 저해하여 HR 활동을 증가시키도록 했다. Microinjection 을 통해 Mouse Rosa26 locus 에 110bp nucleotide (loxP-Multi Cloning Site-loxP2272)를 KI 시킬 때, KEAP1 의 저해 유무에 따라 상대적인 KI 효율이 달라짐을 확인했다 (test 35.7% vs control 23.9%). 더 나아가, UPF1 loxP floxed 마우스 제작을 위해 타겟 위치에 여러 개의 sgRNA 를 겹치도록 설계한 결과, 겹치지 않았을 때와 비교했을 때 약 3 배의 KI 효율 증가를 확인하였다. 무엇보다도 Morc2a gene 의 cC260t single nucleotide morphism (SNP)를 포함한 마우스 제작 실험에서 overlapping sgRNAs 와 KEAP1 inhibition 을 처리한 결과 KI 효율이 0-35.7%까지 큰 차이를 보였다. 본 연구에서는 3 가지의 실험을 통해 overlapping sgRNA 와 KEAP1 저해가 정밀한 KI 효율을 증가시키고 KI 동물 제작에 유용함을 입증하고자 한다.

다음으로는 과민성 대장 증후군 (IBS)을 위한 동물 모델에 대한 연구를 진행하였다.

과민성 대장 증후군은 현대인들의 약 10~20%가 겪고 있는 흔한 소화기 질환으로 구조상 원인은 없지만 식사나 가벼운 스트레스 후 복통, 복부 팽만감과 같은 불쾌한 소화기 증상이 반복되며 설사 혹은 변비 등의 배변장애 증상을 보이는 만성적인 질환이다.

이 연구에서는 brain-gut interaction 을 가장 잘 연구할 수 있는 stress 를 유발시켜 만드는 모델을 이용했다. Early-life stress 는 IBS 의 주요한 원인 중 하나로, 과민성대장증후군 모델을 만들기 위해 C57BL/6 mouse 를 대상으로 생후 3 일 차부터 14 일 차까지 어미와 하루 3 시간 동안 분리하여 과민성대장증후군을 유도하였다.

NMS 로 인한 stress 를 측정하기 위해 Tyrosine Hydroxylas (TH) 유전자 발현을 부신 피질에서 확인하였다. 그리고 NMS stress 를 받은 C57BL/6 의 분변 수분 함량 측정을 통해 IBS-D 유형임을 확인하였다 (NMS 14.67%: control 7.65% at 12weeks). 몸무게 측정 결과 성장 차이는 보이지 않았다. 또한, 여러 종의 NMS 군과 control 군의 염증 병변을 확인하기 위해 F4/80, Gr1, CD3, mast cell chymase 를 IHC 를 통해 확인하였고, qPCR 로 TLRs, inflammatory cytokine genes 의 mRNA expression 측정 결과 NMS 와 control group 에서 큰 차이가 나타나지 않았다. 특이점으로는 H&E 와 IHC 실험 결과에서 장운동세포 ICC 의 마커인 *c-kit* 이 NMS group 에서 높게 발현되었고, 이는 NMS 를 통한 stress 유발이 장운동세포인 ICC 를 활성화하여 장운동을 촉진시킨다는 것을 유추할 수 있다. 이를 확인하기 위해 또다른 신경 전달 세포 물질인 nNOS 를 장에서 확인해본 결과, 대조군에 비해 실험군에서 nNOS 발현이 확연히 높음을 확인하였다. 반대로, nNOS 가 발현되지 않는 C57BL/6.nNOS-/- mouse 에서 IBS 유형을 확인해본 결과 IBS-C(NMS 7.76%: control 11.96%) 유형임을 확인하였다. 즉, C57BL/6 는 NMS 실험을 통해 human IBS-D 모델, nNOS deficient mice 는 IBS-C 모델로 적합한 것으로 보인다. 본 연구에서 가장 중요한 발견은 *c-kit* 과 nNOS 가 스트레스로 유도되는 ICC 활성의 좋은 마커가 될 수 있음을 보여준 것이다.

결론적으로, 이 연구를 통해 overlapping sgRNA 를 통한 KI 효율 향상 방법 설립과 IBS 의 바이오마커를 발견하였다.